THE JOURNAL OF PHYSICAL CHEMISTRY B

Article

pubs.acs.org/JPCB

A SAXS Study of Aggregation in the Synergistic TBP–HDBP Solvent Extraction System

Ross J. Ellis,*[,†] Timothy L. Anderson,[‡] Mark R. Antonio,[†] Alex Braatz,[‡] and Mikael Nilsson*[,‡]

[†]Chemical Sciences and Engineering Division, Argonne National Laboratory, 9700 South Cass Avenue, Argonne, Illinois 60439-4831, United States

[‡]Department of Chemical Engineering and Materials Science, University of California Irvine, 916 Engineering Tower, Irvine, California 92697-2575, United States

ABSTRACT: The macroscopic phase behaviors of a solvent system containing two extractants, tri-*n*-butyl phosphate (TBP) and di-*n*-butyl phosphoric acid (HDBP) in *n*-dodecane, were investigated through use of liquid–liquid extraction and small-angle X-ray scattering (SAXS) experiments. Five organic solutions, each containing a total extractant concentration (TBP + HDBP) of 1 M in varying molar ratios (0, 0.25, 0.5, 0.75, and 1.0 [TBP]:[TBP + HDBP]), were contacted with 0.2 M HNO_3 aqueous solutions without and with dysprosium(III) at a concentration of 10^{-4} M. An enhancement of the extraction of Dy^{3+}—due to effects of synergism arising from the binary combination of extractants—was observed. SAXS data were collected for all solution compositions from 0 to 1 mol-fraction end ratios of TBP after contact with the acidic aqueous solutions both in the absence and presence of Dy as well as for the organic phases before aqueous contact. In the precontacted solutions, no notable changes in the SAXS data were observed upon combining the extractants so that the scattering intensity (I) measured at zero angle (Q = 0 $Å^{-1}$)—parameter $I(0)$—the experimental radius of gyration (R_g), and the maximum linear extent (MLE) of the extractant aggregates were arithmetic averages of the two end members, 1 M HDBP, on the one hand, and 1 M TBP, on the other. In contrast, after contact with the aqueous phases with and without Dy^{3+}, a significant reorganization occurs with larger aggregates apparent in the extractant mixtures and smaller in the two end member solutions. In particular, the maximum values of the metrical parameters ($I(0)$, R_g, and MLE) correlate with the apparent optimal synergistic extraction mole ratio of 0.25. The SAXS data were further analyzed using the recently developed generalized indirect Fourier transformation (GIFT) method to provide pair-distance distribution functions with real-space information on aggregate morphology. Before aqueous contact, the organic phases show a systematically varying response from globular-like reverse micelles in the case of 1 M TBP to rod-shaped architectures in the case of 1 M HDBP. After aqueous contact, the aggregate morphologies of the mixed extractant systems are not simple linear combinations of those for the two end members. Rather, they have larger and more elongated structures, showing sharp discontinuities in the metrics of the aggregate entities that are coincident with the synergistic extraction mixture for Dy^{3+}. The results in this initial study suggest a supramolecular, micellization aspect to synergism that remains underexplored and warrants further investigation, especially as it concerns the contemporary relevance to decades-old process chemistry and practices for high throughput separations systems.

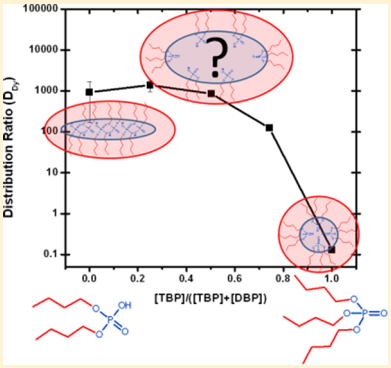

INTRODUCTION

In the diverse field of separations for nonvolatile solutes (e.g., metal ions), there is no hydrometallurgical process more widespread than solvent extraction. It has cross-cutting applications in the pharmaceutical industry,[1] the production of precious metals,[2] base metals,[3] rare-earth elements,[4] and in the chemical treatment of used nuclear fuel.[5] In its essence, the practice of solvent extraction for chemical separation and purification entails the use of a biphasic (liquid–liquid) solution system: an aqueous phase containing a target solute, such as a metal ion, is contacted with an immiscible organic solvent containing a surfactant-like molecule (extractant). The targeted solute is bound selectively by the extractant and is drawn into the organic phase, thus separating it from other aqueous solutes. Often, mixtures of two extractants are used because this imparts enhanced separating properties compared to either extractant on their own and above the simple addition of each component. This phenomenon is known as *synergism* or *synergistic (or synergic) extraction*.[6−9] The synergistic effect occurs in several systems, often combining neutral phosphorus-containing reagents with acidic extractants,[10−14] or related systems.[15] A well-known synergistic system is that of the extractants tri-*n*-butyl phosphate (TBP) and di-*n*-butyl phosphoric acid (HDBP) (Figure 1).[16] TBP has been extensively studied due to its relevance to the PUREX (Plutonium and Uranium Recovery by EXtraction) process, which remains the cornerstone for nuclear fuel reprocessing.[17] Because HDBP is formed by the degradation of TBP during

Received: January 29, 2013
Revised: April 13, 2013
Published: April 16, 2013

   dx.doi.org/10.1021/jp401025e | *J. Phys. Chem. B* 2013, 117, 5916–5924

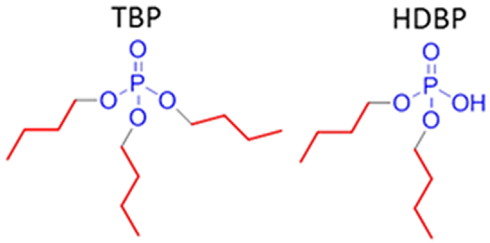

Figure 1. Extractants tri-*n*-butyl phosphate (TBP) and di-*n*-butyl phosphoric acid (HDBP). The polar (hydrophilic) metal binding "head-groups" are highlighted in blue, and the nonpolar (oleophilic) "tail-groups" are highlighted in red.

this process, the extraction behavior in mixtures of these two extractants is important.[13,18−21]

The origins of synergism are not fully understood, and several scenarios involving the formation of binary molecular complexes have been proposed that invoke concepts rooted in the molecular-scale interactions centered on the metal ion.[8−10,22] Thus, in the long-standing separation science tradition, the fundamental driving forces causing synergism when two amphiphilic extractants are mixed have been sought through use of experimental methods in classical metal−ligand coordination chemistry.[22] For example, metrical information and stoichiometric coefficients for extracted metal complexes are readily obtained by combinations of X-ray absorption spectroscopy and time-resolved laser-induced fluorescence spectroscopy[23] as well as kinetics and other physicochemical measurements.[22] Although short-range metal-specific information is valuable and an interesting avenue of research, in our study, synergism in the TBP−HDBP system is approached from a supramolecular (rather than molecular) perspective using X-ray scattering experiments to provide structural information about large-scale assemblies in solution.

Amphiphilic molecules are well-known to self-assemble when dissolved in both apolar and polar solvents, and the resulting macromolecular structures profoundly influence the physical properties of the system.[24] In apolar solvents (e.g., *n*-dodecane) used in solvent extraction processes, amphiphiles assemble to form reverse micelles (RMs) or water-in-oil (W/O) microemulsions.[25−28] These are characterized by polar cores made up from amphiphile head-groups and other hydrophilic moieties (e.g., water, metal ions, acid) surrounded by the apolar amphiphile tail-groups that comprise the oleophilic corona stabilized in a continuous phase of organic solvent. The size and shape of RMs is highly sensitive to the conditions within the system. For example, TBP can form RMs with aggregation numbers ranging from 2 to 5 (Figure 2).[29,30] Varying the mole ratio of two different amphiphiles is an established method of tuning the shape and size of RM-type aggregates.[31−33] Therefore, we are spurred to investigate how varying the mole ratios of TBP and HDBP in an apolar solvent extraction diluent (*n*-dodecane) affects the structure of the resulting aggregates, and how these aggregates might be linked to the physical property of synergism. Indeed, interactions between TBP and HDBP are known and have been reported;[7] however, the impact of these on the nature of self-assembled domains of aggregates and synergism has yet to be investigated.

Our notion that RM aggregates exist in the TBP−HDBP system is well founded in historical literature. Dialkyl phosphoric acid extractants, such as HDBP, HDHP (di-*n*-hexyl phosphoric acid), and HDEHP (di-2-ethylhexyl phosphoric acid), have been long known to assemble into dimers when in hydrocarbon solvents[3,7] and then into large RMs when bound to metal ions.[34−37] This behavior is coming to be recognized to have a profound importance in the extractive properties of practical systems, highlighted by recent studies of the aggregation behaviors in the TRUEX[38] and DIAMEX-SANEX[39,40] processes. Neutral extractants too, including TBP, are especially prone to forming RMs,[41−47] and the use of small-angle X-ray (SAXS) and neutron (SANS) scattering techniques[48,49] to explore the structures and interactions between RM aggregates, and correlating the metrical details (such as the RM radius of gyration, R_g, and shape) with extractive and physical properties is legion. We used SAXS to investigate the effect of varying mole ratios of TBP and HDBP in the *mixed* system on the aggregated structure. Our hypothesis was that, as in other mixed amphiphile RM systems,[31−33] the structures produced by the extractant mixtures would be different compared to the extractants on their own. We then sought to identify whether there was any correlation between the solution structure at different TBP−HDBP mole ratios and the synergistic behavior with regard to the extraction of dysprosium, a non-redox-active trivalent ion (Dy^{3+}) near the middle of the lanthanide series ($Z = 66$) with convenient activation properties for quantitative analyses. Whereas the work presented here focuses on the X-ray scattering phenomena, more details on the extraction data and its interpretation are presented in a parallel study.[50]

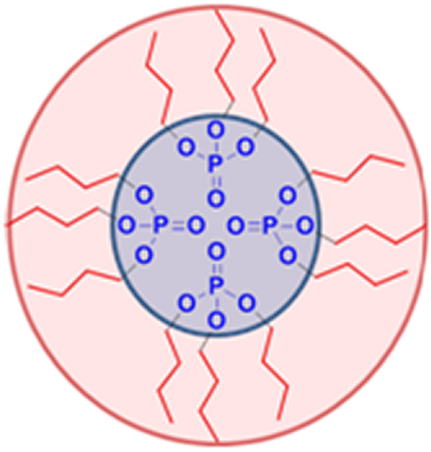

Figure 2. Depiction of a reverse micelle made up from four TBP molecules.[29] The oleophilic tail-groups (red) comprise the nonpolar corona that surrounds a polar core consisting of the hydrophilic head-groups and solutes, such as water, acid, and metal ions.

In a recent seminal study of a similar synergistic solvent extraction involving a dialkyl phosphoric acid (HDEHP) and a neutral extractant (tri-*n*-octyl phosphine oxide, TOPO), Dourdain et al. demonstrated a relationship between aggregation and synergism.[51] They found that the free energy of aggregation necessary to form mixed RMs was correlated with peak synergy, suggesting that synergism may be rooted in architectures formed on the supramolecular scale (RMs) and not wholly on the molecular scale of metal−extractant interactions. However, contrary to what might be expected, they observed no relationship between the *structure* (form) of these mixed aggregates and synergy; i.e., the aggregates formed in the mixed HDEHP−TOPO extraction system were no more than just the average of the end members HDEHP and TOPO on their own.

dx.doi.org/10.1021/jp401025e | J. Phys. Chem. B 2013, 117, 5916−5924

In the present study, we investigate the aggregate assemblies formed in the TBP–HDBP synergistic system, focusing our investigation on SAXS. SAXS is sensitive to the difference in electron density between the RM cores and the surrounding hydrocarbon corona and solvent so that the scattering pattern provides a direct window into the form of the aggregates. We used a variety of different techniques, including the recently developed generalized indirect Fourier transformation (GIFT) method (see below), to interpret the SAXS data and to provide new information on the mixed domain structures of RMs.

EXPERIMENTAL SECTION

The extraction of Dy^{3+} into the organic phase was carefully monitored as a function of TBP:HDBP mole ratio and related to aggregation, which was, in turn, probed through use of SAXS.

Extraction Experiments. Liquid–liquid extraction experiments using TBP and HDBP in various ratios in *n*-dodecane were carried out at room temperature. An aqueous solution of 10^{-4} M Dy^{3+} (chosen for ease of elemental analysis by using neutron activation and because Dy^{3+} is an analogue for other trivalent lanthanides present in used nuclear fuel) in 0.2 M HNO_3 + 1.8 M NH_4NO_3 (a total of 2 M nitrate) was prepared for solvent extraction experiments. Organic solutions contained a total of 1 M extractant concentration (TBP + HDBP) but in varying molar ratios (1.0 M:0 M, 0.75 M:0.25 M, 0.5 M:0.5 M, 0.25 M:0.75 M, and 0 M:1.0 M; TBP:HDBP). The *n*-dodecane was obtained from Alfa Aesar with >99% purity, the TBP was obtained from Acros Organic with >99% purity, and the HDBP from Aldrich with >97% purity. The organic chemicals were all used without any further purification. The TBP and HDBP were checked for impurities using an in-house gas chromatography method, and it was found that the TBP had 0.1% HDBP as the only impurity. The HDBP contained 2% TBP and less than 1% H_2MBP (mono-*n*-butyl phosphate). These impurities were accounted for in the calculations of the final TBP:HDBP ratios used. The H_2MBP was assumed to be removed in the pre-equilibration step as described below. HDBP solubility in the aqueous phase may be non-negligible depending on the conditions used, e.g., the pH of the aqueous phase; however, under the conditions used in this work, HDBP was assumed to remain in the organic phase. An experiment comparing purified HDBP by the copper precipitation method[52] to nontreated HDBP, as in the work presented in this paper, showed no difference between the distribution of dysprosium(III) and water at 10^{-4} M metal ion concentration and using similar organic and aqueous phases as in this work. A Dy^{3+} stock solution was obtained by dissolving dysprosium oxide, 99.999% (Dy_2O_3) provided by Michigan Metals & Manufacturing, in nitric acid. This solution was subsequently standardized for its Dy^{3+} concentration, acidity, and excess nitrate concentration by a combination of neutron activation analysis, ion exchange, and potentiometric titration. Concentrated nitric acid (15.8 M) was supplied by Fisher Scientific. Ammonium nitrate solutions to adjust salt concentration were made by recrystallization of the solid salt supplied by Fisher Scientific. Water used to dilute concentrated solutions was obtained from an in-house source of ultrapure (18.2 MΩ-cm) water. The aqueous phase was pre-equilibrated by contacting with an equal volume of pure *n*-dodecane for 15 min, followed by centrifugation to separate the phases. The organic phases were pre-equilibrated by contacting with an equal volume of aqueous solution containing ammonium nitrate and nitric acid equivalent to the aqueous phase that the organic phase would be extracting from but without the dysprosium ion. The pre-equilibration was carried out to ensure that each phase would be saturated, i.e., the aqueous phase saturated by *n*-dodecane and the organic saturated by H_2O and HNO_3, to avoid volume changes during the metal extraction. Samples of the pre-equilibrated organic phases were taken to observe any water and acid uptake in the absence of dysprosium, and for SAXS measurement (organic phases only). Samples of the non-pre-equilibrated, simple mixtures of TBP and HDBP in *n*-dodecane (i.e., the so-called "dry" organic phases) were used as reference solutions for SAXS measurements, and to provide a baseline for water and acid uptake. Samples of the non-pre-equilibrated aqueous phase containing Dy^{3+} were analyzed to provide the initial Dy and nitric acid concentrations using neutron activation analysis, potentiometric titrations, and ion chromatography (for total nitrate concentration). This initial Dy solution was used for extraction by the contact of equal volumes of aqueous and organic phases for 15 min by vigorous shaking on a vortex mixer followed by 5 min of centrifugation. Samples of each phase were taken for Dy analysis. The remainder of the organic phase was taken for water content analysis, by Karl Fischer titrations (Metrohm model 831 KF Coulometer), and for SAXS measurements. The metal concentration was measured by neutron activation analysis using the UC Irvine 250 kW TRIGA reactor. The dysprosium in the sample was activated (to produce ^{165}Dy), and the sample was measured on a Canberra HPGe detector utilizing the major gamma-emission at ~94.7 keV for analysis. The concentrations of the resulting organic solutions that were analyzed using SAXS are given in Table 1.

Table 1. Concentrations of Organic Phases after Contact with Aqueous Dy^{3+} Solutions

$[TBP]^a$ (M)	$[HDBP]^a$ (M)	$[H_2O]_{org}$ (M)	$[Dy]_{org}$ (M)
1.00(6)	0.00(1)	0.36	1.15×10^{-5}
0.75(8)	0.24(8)	0.41	9.92×10^{-5}
0.51(2)	0.49(2)	0.43	9.99×10^{-5}
0.26(5)	0.73(1)	0.41	9.99×10^{-5}
0.01(6)	0.98(1)	0.23	9.99×10^{-5}

[a]The values in parentheses for TBP and HDBP concentrations are the third decimal point of the molar amount and should be considered having a large uncertainty.

SAXS Measurements. SAXS data for the organic phases from the 0.2 M HNO_3 contacts, both with and without Dy^{3+}, as well as for the dry organic solutions were collected at beamline 12-ID-C at the Advanced Photon Source (APS).[53] The incident photon energy was 36.185 keV, providing good X-ray transmittance for all compositions of the solution systems. A single 2 mm diameter quartz capillary tube was used for containment of all solutions, facilitating meaningful comparisons of the SAXS intensities, $I(Q)$, where Q is the momentum transfer ($Å^{-1}$) according to eq 1.

$$Q = \frac{4\pi \sin\theta}{\lambda} \tag{1}$$

Here, 2θ is the scattering angle and λ is the wavelength of the incident X-ray beam. Five 30 s exposures, obtained with a MAR CCD, for each sample (containing data with less than a 1% shot-to-shot variation over all values of momentum transfer, $0.03\ Å^{-1} \le Q \le 0.86\ Å^{-1}$) were averaged, and the background-

dx.doi.org/10.1021/jp401025e | J. Phys. Chem. B 2013, 117, 5916–5924

subtracted data were analyzed following standard procedures.[39,54]

SAXS Data Interpretation. In the absence of aggregation, the extractant monomers produce only weak scattering that is barely discernible above the solvent background. As RM aggregates form, each molecule participates in the scattering by the square of the volume of the micelles so that the supramolecular structure (and not the molecular structure of the numerous monomers) dominates the SAXS data.[55] The radius of gyration, R_g (a shape-independent measure of particle size in terms of the root mean square of all distances in a particle from its center of mass[48]), of the scattering particles and the scattering intensity at zero momentum transfer, $I(0)$, were determined from the GIFT fits to the entire scattering curves. The analysis of the low Q data alone using the Guinier approximation was vitiated by the curvature of the Guinier plots, $\log(I(Q))$ vs Q^2, which is indicative of structure factor interference and therefore does not give accurate R_g.[48]

The GIFT method[56−58] was used to obtain $p(r)$ functions (structure information in real space) from scattering data in Q space. GIFT interprets the globular particle system, $I(Q) = nP(Q)S(Q)$, where $P(Q)$ is the average form factor (corresponding to the shape and size of the scattering particles), $S(Q)$ is the average structure factor (from interparticle interactions), and n is the number of particles per unit volume. $P(Q)$ is the Fourier transformation of its real space counterpart, $p(r)$, according to eq 2:

$$P(Q) = 4\pi \int_0^\infty p(r) \frac{\sin Qr}{Qr} \, dr \tag{2}$$

This means that, to deduce $p(r)$, the inverse Fourier transformation (IFT) of an experimental $P(Q)$ must be calculated. In concentrated interacting systems, such as those involved in solvent extraction, the structure factor, $S(Q)$, must be modeled and subtracted from the scattering data, $I(Q)$, to give $P(Q)$ from which $p(r)$ is derived. The selection of the appropriate structure factor model is key to achieving coherent $p(r)$ functions from GIFT, and the model selected in the present study was the Percus−Yevick (PY) closure relation[59] that has been shown to closely approximate the interaction effects of micelles in SAXS studies from numerous solvent extraction systems.[39,43,44,46,60]

The PY closure relation for hard spheres solves the Ornstein−Zernicke equation on the principle that the hard sphere potential is zero if the particles do not overlap and infinity if they do (approximating the structure factor that results from the excluded volume effect). The resulting structure factor depends on the radius and volume fraction of particles, with a modification to include polydispersity with a distribution function. The PY closure relation structure factor is simple, is fast, and can even be used for non-hard-sphere interaction potentials, as many potentials behave similarly to effective hard spheres.[61] According to Glatter,[62] this structure factor model holds true for deviations from hard spheres and for deviations from perfect spherical symmetry, soliciting its use to evaluate scattering data of interacting elongated particles. This has been demonstrated in a string of recent publications by Glatter and Shrestha et al., who used the GIFT in combination with the PY closure relation to interpret SAXS data from interacting nonionic surfactant reverse micelle systems in nonpolar media (similar to solvent extraction organic phases).[31−33,63] These studies were effective in showing the growth of spherical particles into elongated worm-like aggregates. A detailed discussion of the PY closure relation model in the GIFT treatment of SAXS data is given in a recent review article by Fritz and Glatter.[62]

RESULTS AND DISCUSSION

Solvent extraction experiments were performed to define the macroscopic phase behaviors of the system by varying the mole ratio of TBP:HDBP (keeping the total extractant concentration constant at 1 M) and contacting with a 0.2 M HNO_3 aqueous solution containing 10^{-4} M Dy^{3+}. Figure 3 shows how the distribution ratio of Dy^{3+}, defined as the ratio of the analytical concentrations of the metal ion in the organic and aqueous phases, varies with TBP:HDBP mole ratio. A nonlinear trend for Dy^{3+} uptake is observed, indicating a synergistic effect between the TBP and HDBP extractants. The data of Figure 3 shows that the *average* distribution ratio for dysprosium, D_{Dy}, peaks at 25% TBP (0.25 M TBP + 0.75 M HDBP), suggesting an optimal extraction mixture at approximately this value. Thereafter, the Dy distribution ratio is essentially constant, showing a slight decrease to 75% TBP, after which is a significant decrease to the end system of 100% (1 M) TBP. In the absence of synergism, the D_{Dy} values for ideal solutions with binary mixtures of extractants are expected to vary more linearly between the 0 and 1.0 mol fractions. The black dotted line in Figure 3 shows the trend that might be expected for simple additive extraction behaviors in the absence of synergism.

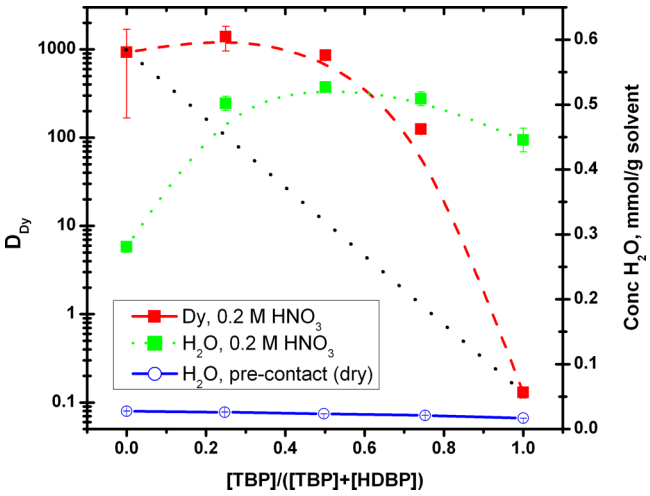

Figure 3. Distribution ratios of dysprosium (red) and concentration of water in the organic phase vs TBP:HDBP mole ratio before (blue) and after (green) contact with 0.2 M HNO_3 + 1.8 M NH_4NO_3 aqueous phases containing 10^{-4} M Dy^{3+}. The error bars represent standard deviations from triplicate measurements. The black dotted line shows the trend expected for simple additive extraction behaviors on D_{Dy} in the absence of synergism. The lines in the figure do not represent fits to the data; they simply serve as guides for the reader. Note: A small amount of nitric acid also extracts, increasing linearly with TBP mole ratio. This is addressed in a separate study from our lab.[50]

Figure 3 also shows how the water content in the organic phase changes across the series (green). Again, a nonlinear trend is observed that peaks for the extractant mixture at 50% TBP (0.5 M TBP + 0.5 M HDBP). It is worth noting here that at this mixture the largest deviation from the dotted line is observed for D_{Dy}. The amount of water found in the organic solutions before contact (i.e., "dry" organic phases) is shown in Figure 3 as well (blue). The amount present before contact is as

dx.doi.org/10.1021/jp401025e | J. Phys. Chem. B 2013, 117, 5916−5924

least 1 order of magnitude lower than that after contact. Elevated water content is indicative of RM or microemulsion structural growth;[49] all of the extractant mixtures (0.25, 0.5, and 0.75 [TBP]/([TBP] + [HDBP])) show increased water concentrations compared to either of the end member solutions, 1 M HDBP and 1 M TBP. To investigate the nature of the water-laden aggregates formed in the organic phases as a function of the TBP:HDBP compositions, SAXS measurements were collected from all of the solutions before contact and after contact with 0.2 M HNO_3 aqueous phases with and without Dy^{3+}. As shown in Figure 4, the scattering intensities, $I(Q)$ vs

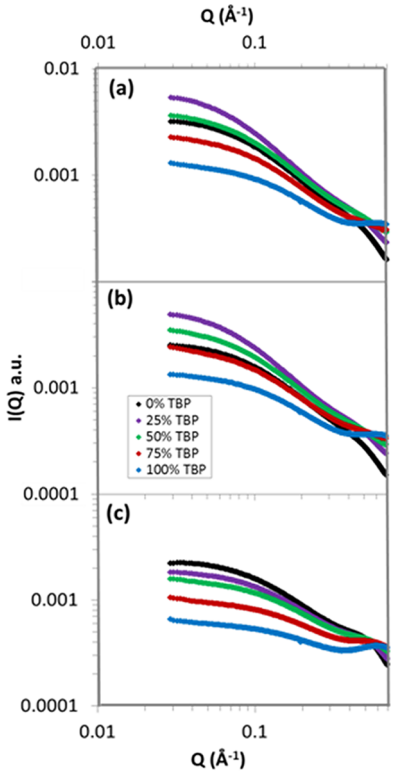

Figure 4. Log–log plot of the SAXS data for the three TBP:HDBP mixtures and the two individual extractant solutions after contact with 0.2 M HNO_3 + 1.8 M NH_4NO_3 aqueous phases (a) without Dy and (b) with 10^{-4} M Dy^{3+}. The responses for the pre-aqueous-contact ("dry") organic solutions are shown in part c. The data for the solutions with [TBP]:[TBP + HDBP] mole ratios of 0, 0.25, 0.5, 0.75, and 1.0 are shown as black, purple, green, red, and blue lines, respectively.

Q, varied with the molar ratios of the extractants. The SAXS data for the systems without Dy^{3+} (a) and with Dy^{3+} (b) are essentially identical, showing that extraction of the metal ion, in this case, has very little impact on the macromolecular organic phase structure, as expected at these low concentrations of Dy^{3+}. The scattering curves for the contacted solutions, (a) and (b), are, however, notably different from the precontacted solutions (c) in two respects: (1) The intensities at low Q ($Q \rightarrow I(0)$) are smaller for the precontacted solution. (2) The ordering of scattering intensities among the three extractant mixtures before contact falls between the responses for the two end member solutions in an order that is predictable based upon the arithmetic averages of the extractant concentrations.

For globular systems, such as the RM/microemulsions that comprise solvent extraction organic phases, the intensity at $I(0)$ is dependent on the volume (V) of the core of the aggregates according to eq 3.

$$I(0) = (\phi V \Delta\rho)^2 P(0) S(0) \quad (3)$$

Here, ϕ is the volume fraction of the scattering aggregates, $\Delta\rho$ is the electron density contrast, and $P(0)$ and $S(0)$ are the form and structure factors, respectively, of the aggregates. In the recent study by Dourdain et al.,[51] a predictable change in $I(0)$ was observed between the pure end members, suggesting that there were no notable changes in aggregate state in the mixed HDEHP–TOPO system; i.e., the volume of the aggregates in the mixed system was an approximate arithmetic average of the end members. Such a trend is also observed in the precontacted HDBP–TBP mixtures that are the focus of the present study, with $I(0)$ increasing between 100% TBP and 0% TBP in a linear manner; see the blue line and blue circles in Figure 5a. However, after the organic phases were contacted with the aqueous phases—with or without Dy^{3+}—the trend in $I(0)$ changes so that it peaks at the optimal synergistic mixture of 25% TBP; see red and green squares (and color matching dashed lines) in Figure 5a. This suggests that, after contact, the mixed systems form larger micelles, with a different aggregated structure than the end members, or that the structure factor $S(Q)$ has changed across the series. This behavior is different from that observed in the aforementioned study by Dourdain et al.[51]

Metrical information about the aggregates without Dy (green squares) and with Dy (red squares) is provided in Figure 5b in terms of R_g values, which are plotted as a function of the mixing ratio of the extractants. The corresponding results for the precontacted solutions (blue circles) show that the system ordering is described by a simple linear combination of the responses of the two end members (blue line). This is not true for the contacted phases where the R_g values peak at 19.3–20 Å between the two end member solutions at an extractant molar ratio of 0.25. The variation in the experimentally determined R_g values clearly shows that, after contact with the aqueous phase, the particle scatterers assemble into larger entities in the mixed extractant phases than in either of the single component systems. It is noteworthy that the peak R_g value in the synergistic 0.25 M acid systems corresponds to the optimum TBP mole ratio for the uptake of Dy^{3+} (Figure 3), so that aggregate size and extraction efficiency appear to be correlated.

Additional information about the morphology of the aggregates comes from the $p(r)$ functions, shown in Figure 6, obtained by the GIFT treatment of the SAXS data. The extended, tail-like decay of the $p(r)$ functions indicates elongated RMs that vary from globular/ellipsoid to cylindrical.[64,65] In the precontacted organic phases (c), the tail becomes steadily more pronounced as the mole ratio of TBP decreases and HDBP increases, indicating an elongation of micelles from globular in the case of 1 M TBP to more rod-shaped in the case for 1 M HDBP. The postcontact $p(r)$ functions have a different ordering across the series with the mixed systems showing larger, more elongated structures than the end members.

The point at which the $p(r)$ functions decay to zero (r_{max}) corresponds to the maximum linear extent (MLE) of the aggregates or the length of the rod. The variation of the MLE values for each of the five extractant mole ratios is shown in Figure 7. The largest MLE values (90–100 Å) are observed at the 0.25 extractant ratio, both without Dy (green squares) and with Dy (red squares). The domed nature of the MLE variation

dx.doi.org/10.1021/jp401025e | J. Phys. Chem. B 2013, 117, 5916–5924

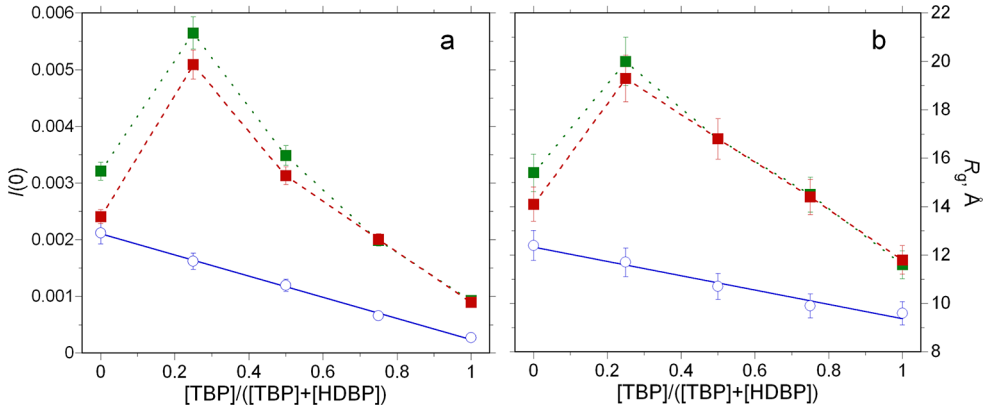

Figure 5. (a) $I(0)$ and (b) radius of gyration (R_g, Å) calculated from the entire scattering curves for the organic phases containing varying ratios of TBP and HDBP with constant (1 M) extractant concentrations after contact with 0.2 M HNO_3 + 1.8 M NH_4NO_3 aqueous phases without Dy (green squares) and with Dy^{3+} (red squares). The linear response of the precontact ("dry") organic phases (blue circles and line) is typical for ideal mixing behavior without either synergism or antagonism of solution properties.

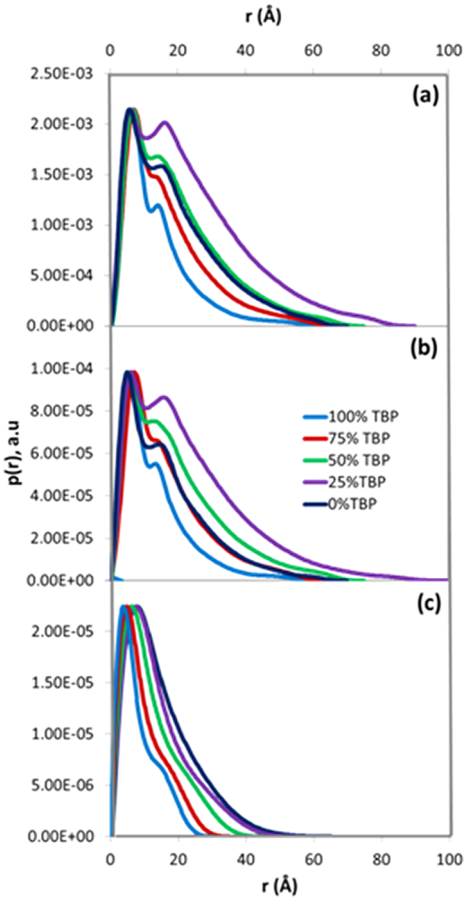

Figure 6. $p(r)$ functions for the organic phases contacted with 0.2 M HNO_3 + 1.8 M NH_4NO_3 aqueous phases without Dy^{3+} (a) and with Dy^{3+} (b), and the precontact ("dry") organic phases (c). The data for the solutions with TBP mole ratios of 1, 0.75, 0.50, 0.25, and 0.0 are shown with the same colors as in Figure 4. The maximum linear extent (MLE) of the tails corresponds to r_{max}.

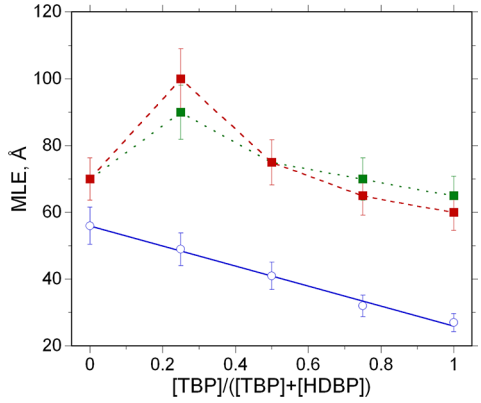

Figure 7. Maximum linear extent obtained from the PDDFs for the organic solutions containing varying ratios of TBP and HDBP with constant (1 M) extractant concentrations after contact with 0.2 M HNO_3 + 1.8 M NH_4NO_3 aqueous phases without Dy^{3+} (green squares) and with Dy^{3+} (red squares). The linear response of the dry organic phases (blue circles and line) is typical for ideal mixing behavior without either synergism or antagonism of solution properties.

with the extractant ratio shows, once again, that the system behaviors with mixed TBP and HDBP extractants after aqueous contact are not simple arithmetic averages of the responses for the two end members, like it is for the precontacted solutions (see blue circles and line).

A notable feature of the $p(r)$ plots is the development of the second peak that is most prominent at the synergistic mixture of 0.25 mol ratio TBP. In analogous studies of nonionic surfactant micelles in aqueous[58] and oil[33] diluents, similar secondary peaks were observed in the GIFT-generated $p(r)$ plots. In these studies, this feature was attributed to interactions between the rod-shaped aggregates that come about as the solution becomes more structured.

Our study agrees with the pioneering work by Osseo-Asare, who showed an enhanced extraction using microemulsions,[66] and by the more recent work by Dourdain et al. that aggregation and synergy are connected.[51] The SAXS results in the precontacted organic phases show that mixing of the two extractants does not result in any notable difference in aggregate structure than just a weighted-arithmetic sum of the member components, as was observed by Dourdain et al.[51] However, after contact with the acidic aqueous phase, significant rearrangement of the organic phase superstructure occurs, with increased ordering and larger aggregates evident in the mixed systems relative to the end members, an effect that was not noted beforehand.[51] Of significant interest is the

dx.doi.org/10.1021/jp401025e | J. Phys. Chem. B 2013, 117, 5916−5924

coincidence of the largest aggregates and the apparent optimal extraction occurring at the same 0.25 TBP mole fraction, suggesting, for the first time, a correlation between aggregate *size* and synergy.

Solvent extraction systems are highly complex and involve interactions on the atomic, molecular, and supramolecular scales that profoundly influence the delicate balance of energetics that underpin metal extraction. Although this study shows a correlation between the aggregated structure and synergistic properties, it does not challenge the traditional molecular-level (coordination chemistry) understanding of synergistic systems. The metal coordination environment, we suspect, is intrinsically connected in the structural hierarchy to the nano- and mesoscale morphologies of the aggregates in ways that are not fully understood. We therefore plan an imminent investigation into how the structural scales are interconnected in the TBP−HDBP system and how they affect the solvent extraction of metal ions, a process that is coordination chemistry at the most fundamental level.[67,68] Nonetheless, the conventional understanding of synergistic extraction in terms of effectively dehydrating a metal ion,[6−9] thereby making the metal−extractant complex more oleophilic, does not harmonize with the water uptake, distribution results, and RM solution structures reported here.

The results of our water and Dy^{3+} analyses as well as SAXS suggest that the effects of micellization may trump the influences of the metal dehydration reaction. The lines of evidence are as follows: A diagnostic indicator of micellization in apolar solutions is the presence of large concentrations of water. The data of Figure 3 show approximately 0.5 mmol/g of H_2O for the three binary TBP−HDBP compositions. These values are larger than those for either TBP or HDBP when used independently, exactly as all of the metrical parameters for the mixtures obtained from SAXS are larger than for either TBP or HDBP. Taken together, the data indicate the formation of large RM aggregates in the organic mixtures. The presence of RMs is directly correlated with the enhancement of H_2O *and* Dy^{3+} extraction, where the optimal stoichiometric extractant combination of 0.25 M TBP + 0.75 M HDBP may provide an environment well suited to accommodate a charge-neutral complex of the Dy^{3+} ion. The formation of RMs by the mixture of extractants (even in the absence of Dy^{3+}) facilitates the synergism of Dy^{3+} extraction in an energetically favorable manner that is ancillary to reactions involving $Dy-OH_2$ bond breaking or HDBP displacement and Dy−TBP bond formation. The Dy-centric, molecular perspectives of synergism complement our central tenet of a supramolecular aspect to synergism. Moreover, the metrical results obtained from the SAXS data presented here are of insufficient resolution to provide insights about the coordination chemistry of Dy^{3+}. Nevertheless, the supramolecular solution structure properties and the high water concentration in the optimum combination of extractants correlate with the observed synergism of Dy^{3+} extraction, wherein D_{Dy} (0.25 M TBP + 0.75 M HDBP) is much greater than the weighted-arithmetic sum of D_{Dy} (TBP) and D_{Dy} (HDBP).

CONCLUSIONS

We observed a synergistic effect in the extraction of dysprosium(III) from an acidic nitrate aqueous phase with a binary extractant system consisting of TBP and HDBP in *n*-dodecane. SAXS data were collected for all system compositions, from the 0 to 1 mol-fraction end ratios [TBP]/([TBP] + [HDBP]) for the precontacted organic phases as well as postcontacted ones with acidic aqueous solutions both with and without Dy^{3+}. In the precontacted solutions, no notable change was observed upon mixing the extractants so that the supramolecular structural metrics—in terms of $I(0)$, R_g, MLE—were arithmetic averages of the two end member solutions (HDBP and TBP). After contact with the aqueous phase (with or without metal ion), a significant reordering occurs in the mixed systems with the largest RM aggregates observed at the optimal TBP mole ratio of 0.25. We show that the correlation between synergism and aggregation, observed in the recent Dourdain et al. study with mixtures of HDEHP and TOPO,[51] also occurs with mixtures of HDBP and TBP, and that a micellization mechanism of synergism is a likely scenario compared to the conventional metal-centric one described by a synergist-driven (here TBP) dehydration of the inner coordination sphere of water in an organic-phase metal−extractant complex. In addition to this, we observe a reordering of the mixed system upon aqueous contact that causes larger aggregates to form in the more synergistic mixtures. The deliberate and rational control of the long-range structural effects observed here for Dy^{3+} may provide a new entry into the manipulation of chemical and physical factors that impact self- and directed-formation of microemulsions in myriad practical process chemistries, in general, and for the PUREX system, in particular.

AUTHOR INFORMATION

Corresponding Author

*E-mail: rellis@anl.gov (R.J.E.); nilssonm@uci.edu (M.N.). Phone: 630-252-3647 (R.J.E.); 949-824-2800 (M.N.).

Notes

The authors declare no competing financial interest.

ACKNOWLEDGMENTS

The authors wish to thank the U.S. Department of Energy through the Nuclear Energy University Program, NEUP Contract No. 120569 and DE-NE0000156 for financial support for the experiments and for the HPGe detector, respectively. The work at Argonne and the use of the Advanced Photon Source are supported by the U.S. Department of Energy, Office of Science, Office of Basic Energy Sciences, Division of Chemical Sciences, Biosciences and Geosciences, under Contract No. DE-AC02-06CH11357.

REFERENCES

(1) Grodowska, K.; Parczewski, A. Organic Solvents in the Pharmaceutical Industry. *Acta Pol. Pharm.* **2010**, *67*, 3−12.

(2) Bernardis, F. L.; Grant, R. A.; Sherrington, D. C. A Review of Methods of Separation of the Platinum-Group Metals through their Chloro-Complexes. *React. Funct. Polym.* **2005**, *65*, 205−217.

(3) Tasker, P. A.; Plieger, P. G.; West, L. C. In *Comprehensive Coordination Chemistry II*; Ward, M. D., Ed.; Elsevier Ltd.: New York, 2004; Vol. *9*, pp 759−808.

(4) Bautista, R. G. In *Handbook on the Physics and Chemistry of Rare Earths*; Gschneidner, K. A., Eyring, L., Eds.; North-Holland: Amsterdam, The Netherlands, 1995; Vol. *21*, pp 1−27.

(5) Musikas, C.; Schulz, W. W.; Liljenzin, J.-O. In *Solvent Extraction Principles and Practice*, 2nd ed.; Rydberg, J., Ed.; Marcel Dekker, Inc.: New York, 2004; pp 507−557.

(6) Ramakrishna, V. V.; Patil, S. K. Synergic Extraction of Actinides. *Struct. Bonding (Berlin)* **1984**, *56*, 35−90.

(7) Kolarik, Z. Interactions of Acidic Organophosphorus Extractants in the Organic Phase. *Solvent Extr. Rev.* **1971**, *1*, 1−62.

(8) Kassierer, E. F.; Kertes, A. S. Displacement of Water in Synergic Extraction Systems. *J. Inorg. Nucl. Chem.* **1972**, *34*, 778−780.
(9) Marcus, Y.; Kertes, A. S. *Ion Exchange and Solvent Extraction of Metal Complexes*; Wiley-Interscience: London, UK, 1969.
(10) Irving, H.; Edgington, D. N. Synergic Effects in the Solvent Extraction of the Actinides. I. Uranium(VI). *J. Inorg. Nucl. Chem.* **1960**, *15*, 158−170.
(11) Irving, H. M. N. H. Synergism in the Solvent Extraction of Metal Chelates. *Solvent Extr. Chem., Proc. Int. Conf.* **1967**, 91−110.
(12) Zangen, M. Some Aspects of Synergism in Solvent Extraction. II. Some Di-, Tri- and Tetravalent Metal Ions. *J. Inorg. Nucl. Chem.* **1963**, *25*, 1051−1063.
(13) Dyrssen, D.; Kuca, L. The Extraction of Uranium(VI) with DBP in the Presence of TBP. The Synergic Effect: Substitution or Addition? *Acta Chem. Scand.* **1960**, *14*, 1945−1956.
(14) Shmidt, O. V.; Zilberman, B. Y.; Fedorov, Y. S.; Palenik, Y. V.; Goletskii, N. D.; Stepanov, A. I. Effect of TBP on Extraction of REE and TPE from Nitric Acid Solutions with Dibutylphosphoric Acid and Its Zirconium Salt. *Radiochemistry (Moscow, Russ. Fed.)* **2003**, *45*, 596−601.
(15) Hagstrom, I.; Spjuth, L.; Enarsson, A.; Liljenzin, J. O.; Skalberg, M.; Hudson, M. J.; Iveson, P. B.; Madic, C.; Cordier, P. Y.; Hill, C.; Francois, N. Synergistic Solvent Extraction of Trivalent Americium and Europium by 2-Bromodecanoic Acid and Neutral Nitrogen-Containing Reagents. *Solvent Extr. Ion Exch.* **1999**, *17*, 221−242.
(16) Hahn, H. T.; Wall, E. M. V. Complex Formation in the Dilute Uranyl Nitrate-Nitric Acid- Dibutyl Phosphoric Acid(DBP)-Tributyl Phosphate(TBP)-Amsco System. *J. Inorg. Nucl. Chem.* **1964**, *26*, 191−202.
(17) Choppin, G. R., Khankhasayev, M. K., Plendl, H. S., Eds. *Chemical Separations in Nuclear Waste Management: The State of the Art and a Look to the Future. (Papers presented at an International Workshop held in Prague, Sept 11, 2000)*; Battelle Press: Columbus, OH, 2002.
(18) Fedorov, Y. S.; Zilberman, B. Y.; Kulikov, S. M.; Blazheva, I. V.; Mishin, E. N.; Wallwork, A. L.; Denniss, I. S.; May, I.; Hill, N. J. Uranium(VI) Extraction by TBP in the Presence of HDBP. *Solvent Extr. Ion Exch.* **1999**, *17*, 243−257.
(19) May, I.; Taylor, R. J.; Wallwork, A. L.; Hastings, J. J.; Fedorov, Y. S.; Zilberman, B. Y.; Mishin, E. N.; Arkhipov, S. A.; Blazheva, I. V.; Poverkova, L. Y.; Livens, F. R.; Charnock, J. M. The Influence of Dibutylphosphate on Actinide Extraction by 30% Tributylphosphate. *Radiochim. Acta* **2000**, *88*, 283−290.
(20) Liem, D. H. Synergistic Effect in the Extraction of Uranium-233(VI) by Dibutylphosphate (HDBP) in the Presence of Tributylphosphate (TBP) or Trioctylphosphine Oxide (TOPO) in Hexane and Carbon Tetrachloride. *Acta Chem. Scand.* **1968**, *22*, 773−790.
(21) Liem, D. H.; Dryssen, D. Synergistic Effect on the Extraction of 233U(VI) by Dibutylphosphate (DBP) and Tributyl Phosphate (TBP) or Trioctylphosphene Oxide (TOPO). *Acta Chem. Scand.* **1966**, *20*, 272−274.
(22) Rydberg, J., Musikas, C., Choppin, G. R., Eds. *Principles and Practices of Solvent Extraction*; Marcel Dekker, Inc: New York, 1992.
(23) Ellis, R. J.; Meridiano, Y.; Chiarizia, R.; Berthon, L.; Muller, J.; Couston, L.; Antonio, M. R. Periodic Behavior of Lanthanide Coordination within Reverse Micelles. *Chem.—Eur. J.* **2013**, *19*, 2663−2675.
(24) Ekwall, P.; Stenius, P. In *International Review of Science, Physical Chemistry, Series Two*; Kerker, M., Ed.; Butterworth: London, UK, 1975; Vol. 7, pp 215−248.
(25) Eicke, H.-F. Surfactants in Nonpolar Solvents: Aggregation and Micellization. *Top. Curr. Chem.* **1980**, *87*, 85−145.
(26) Eicke, H. F. Aggregation in Surfactant Solutions: Formation and Properties of Micelles and Microemulsions. *Pure Appl. Chem.* **1980**, *52*, 1349−1357.
(27) Eicke, H. F. Properties of Amphiphilic Electrolytes in Nonpolar Solvents. *Pure Appl. Chem.* **1981**, *53*, 1417−1424.
(28) Eicke, H. F.; Markovic, Z. Temperature-Dependent Coalescence in Water-Oil Microemulsions and Phase Transitions to Lyotropic Mesophases. *J. Colloid Interface Sci.* **1981**, *79*, 151−158.
(29) Chiarizia, R.; Nash, K. L.; Jensen, M. P.; Thiyagarajan, P.; Littrell, K. C. Application of the Baxter Model for Hard Spheres with Surface Adhesion to SANS Data for the U(VI)-HNO_3, TBP-*n*-Dodecane System. *Langmuir* **2003**, *19*, 9592−9599.
(30) Nave, S.; Mandin, C.; Martinet, L.; Berthon, L.; Testard, F.; Madic, C.; Zemb, T. Supramolecular Organisation of Tri-*n*-Butyl Phosphate in Organic Diluent on Approaching Third Phase Transition. *Phys. Chem. Chem. Phys.* **2004**, *6*, 799−808.
(31) Sharma, S. C.; Shrestha, R. G.; Shrestha, L. K.; Aramaki, K. Viscoelastic Wormlike Micelles in Mixed Nonionic Fluorocarbon Surfactants and Structural Transition Induced by Oils. *J. Phys. Chem. B* **2009**, *113*, 1615−1622.
(32) Shrestha, L. K.; Shrestha, R. G.; Aramaki, K. Intrinsic Parameters for the Structure Control of Nonionic Reverse Micelles in Styrene: SAXS and Rheometry Studies. *Langmuir* **2011**, *27*, 5862−5873.
(33) Shrestha, L. K.; Yamamoto, M.; Arima, S.; Aramaki, K. Charge-Free Reverse Wormlike Micelles in Nonaqueous Media. *Langmuir* **2011**, *27*, 2340−2348.
(34) Gaonkar, A. G.; Neuman, R. D. Interfacial Activity, Extractant Selectivity, and Reversed Micellization in Hydrometallurgical Liquid/Liquid Extraction Systems. *J. Colloid Interface Sci.* **1987**, *119*, 251−261.
(35) Neuman, R. D.; Zhou, N.; Wu, J.; Jones, M. A.; Gaonkar, A. G.; Park, S. J.; Agrawal, M. L. General Model for Aggregation of Metal-Extractant Complexes in Acidic Organophosphorus Solvent Extraction Systems. *Sep. Sci. Technol.* **1990**, *25*, 1655−1674.
(36) Zhou, N. F.; Wu, J.; Sarathy, P. K.; Liu, F.; Neuman, R. D. Comparison of Aggregates Formed by Acidic Organophosphorous Extractants and Metals (Nickel and Cobalt) in Solvent Extraction. *Process Metall.* **1992**, *7A*, 165−170.
(37) Ben, A. I.; Ober, R.; Nakache, E.; Williams, C. E. A Small Angle X-ray Scattering Investigation of the Structure of a Ternary Water-in-Oil Microemulsion. *Colloids Surf.* **1992**, *69*, 87−97.
(38) Diamond, H.; Thiyagarajan, P.; Horwitz, E. P. Small Angle Neutron Scattering Studies of Praseodymium-CMPO Polymerization. *Solvent Extr. Ion Exch.* **1990**, *8*, 503−513.
(39) Antonio, M. R.; Chiarizia, R.; Gannaz, B.; Berthon, L.; Zorz, N.; Hill, C.; Cote, G. Aggregation in Solvent Extraction Systems Containing a Malonamide, a Dialkylphosphoric Acid and Their Mixtures. *Sep. Sci. Technol.* **2008**, *43*, 2572−2605.
(40) Gannaz, B.; Chiarizia, R.; Antonio, M. R.; Hill, C.; Cote, G. Extraction of Lanthanides(III) and Am(III) by Mixtures of Malonamide and Dialkylphosphoric Acid. *Solvent Extr. Ion Exch.* **2007**, *25*, 313−337.
(41) Osseo-Asare, K. Aggregation, Reversed Micelles, and Microemulsions in Liquid-Liquid- Extraction - The Tri-Normal-Butyl Phosphate-Diluent-Water-Electrolyte System. *Adv. Colloid Interface Sci.* **1991**, *37*, 123−173.
(42) Osseo-Asare, K. In *Metal Separation Technologies Beyond 2000: Integrating Novel Chemistry with Processing*; Liddell, K. C., Chaiko, D. J., Eds.; Minerals, Metals & Materials Soc.: Warrendale, PA, 1999; pp 339−346.
(43) Chiarizia, R.; Jensen, M. P.; Borkowski, M.; Ferraro, J. R.; Thiyagarajan, P.; Littrell, K. C. SANS Study of Third Phase Formation in the U(VI)-HNO_3/TBP-*n*-Dodecane System. *Sep. Sci. Technol.* **2003**, *38*, 3313−3331.
(44) Chiarizia, R.; Jensen, M. P.; Borkowski, M.; Ferraro, J. R.; Thiyagarajan, P.; Littrell, K. C. Third Phase Formation Revisited: The U(VI), HNO_3-TBP, *n*-Dodecane System. *Solvent Extr. Ion Exch.* **2003**, *21*, 1−27.
(45) Chiarizia, R.; Jensen, M. P.; Borkowski, M.; Thiyagarajan, P.; Littrell, K. C. Interpretation of Third Phase Formation in the Th(IV)-HNO_3, TBP-*n*-Octane System with Baxter's "Sticky Spheres" Model. *Solvent Extr. Ion Exch.* **2004**, *22*, 325−351.
(46) Chiarizia, R.; Jensen, M. P.; Rickert, P. G.; Kolarik, Z.; Borkowski, M.; Thiyagarajan, P. Extraction of Zirconium Nitrate by TBP in *n*-Octane: Influence of Cation Type on Third Phase

Formation According to the "Sticky Spheres" Model. *Langmuir* **2004**, *20*, 10798−10808.
(47) Erlinger, C.; Belloni, L.; Zemb, T.; Madic, C. Attractive Interactions Between Reverse Aggregates and Phase Separation in Concentrated Malonamide Extractant Solutions. *Langmuir* **1999**, 2290−2300.
(48) Putnam, C. D.; Hammel, M.; Hura, G. L.; Tainer, J. A. X-ray Solution Scattering (SAXS) Combined with Crystallography and Computation: Defining Accurate Macromolecular Structures, Conformations and Assemblies in Solution. *Q. Rev. Biophys.* **2007**, *40*, 191−285.
(49) Chen, S. H. Small Angle Neutron Scattering Studies of the Structure and Interaction in Micellar and Microemulsion Systems. *Annu. Rev. Phys. Chem.* **1986**, *37*, 351−399.
(50) Anderson, T. L.; B., A.; Ellis, R. J.; Antonio, M. R.; Nilsson, M. Synergistic Extraction of Dysprosium and Aggregate Formation in Solvent Extraction Systems Combining TBP and HDBP. *Solvent Extr. Ion Exch.* **2013**, DOI: 10.1080/07366299.2013.787023.
(51) Dourdain, S.; Hofmeister, I.; Pecheur, O.; Dufreche, J. F.; Turgis, R.; Leydier, A.; Jestin, J.; Testard, F.; Pellet-Rostaing, S.; Zemb, T. Synergism by Coassembly at the Origin of Ion Selectivity in Liquid-Liquid Extraction. *Langmuir* **2012**, *28*, 11319−11328.
(52) Partridge, J. A.; Jensen, R. C. Purification of Bis(2-Ethylhexyl) Hydrogen Phosphate by Precipitation of Copper(II) Bis(2-Ethylhexyl) Phosphate. *J. Inorg. Nucl. Chem.* **1969**, *31*, 2587−2589.
(53) Seifert, S.; Winans, R. E.; Tiede, D. M.; Thiyagarajan, P. Design and Performance of a ASAXS (Anomalous Small Angle X-ray Scattering) Instrument at the Advanced Photon Source. *J. Appl. Crystallogr.* **2000**, *33*, 782−784.
(54) Meridiano, Y.; Berthon, L.; Crozes, X.; Sorel, C.; Dannus, P.; Antonio, M. R.; Chiarizia, R.; Zemb, T. Aggregation in Organic Solutions of Malonamides: Consequences for Water Extraction. *Solvent Extr. Ion Exch.* **2009**, *27*, 607−637.
(55) Guinier, A.; Fournet, G. *Small-Angle Scattering of X-rays*; Wiley: New York, 1955.
(56) Brunner-Popela, J.; Mittelbach, R.; Strey, R.; Schubert, K. V.; Kaler, E. W.; Glatter, O. Small-Angle Scattering of Interacting Particles. III. D_2O-$C_{12}E_5$ Mixtures and Microemulsions with *n*-Octane. *J. Chem. Phys.* **1999**, *110*, 10623−10632.
(57) Fritz, G.; Bergmann, A.; Glatter, O. Evaluation of Small-Angle Scattering Data of Charged Particles Using the Generalized Indirect Fourier Transformation Technique. *J. Chem. Phys.* **2000**, *113*, 9733−9740.
(58) Glatter, O.; Fritz, G.; Lindner, H.; Brunner-Popela, J.; Mittelbach, R.; Strey, R.; Egelhaaf, S. U. Nonionic Micelles near the Critical Point: Micellar Growth and Attractive Interaction. *Langmuir* **2000**, *16*, 8692−8701.
(59) Percus, J. K.; Yevick, G. J. Analysis of Classical Statistical Mechanics by Means of Collective Coordinates. *Phys. Rev.* **1958**, *110*, 1−13.
(60) Chiarizia, R.; Briand, A.; Jensen, M. P.; Thiyagarajan, P. SANS Study of Reverse Micelles Formed upon the Extraction of Inorganic Acids by TBP in *n*-Octane. *Solvent Extr. Ion Exch.* **2008**, *26*, 333−359.
(61) Barker, J. A.; Henderson, D. Perturbation Theory and Equation of State for Fluids. II. A Successful Theory of Liquids. *J. Chem. Phys.* **1967**, *47*, 4714−4721.
(62) Fritz, G.; Glatter, O. Structure and Interaction in Dense Colloidal Systems: Evaluation of Scattering Data by the Generalized Indirect Fourier Transformation Method. *J. Phys.: Condens. Matter* **2006**, *18*, S2403−S2419.
(63) Shrestha, L. K.; Sato, T.; Dulle, M.; Glatter, O.; Aramaki, K. Effect of Lipophilic Tail Architecture and Solvent Engineering on the Structure of Trehalose-Based Nonionic Surfactant Reverse Micelles. *J. Phys. Chem. B* **2010**, *114*, 12008−12017.
(64) Glatter, O. In *Neutrons, X-Rays and Light*; Lindner, P., Zemb, T., Eds.; Elsevier Science B.V.: Amsterdam, The Netherlands, 2002; pp 73−102.
(65) Glatter, O. The Interpretation of Real-Space Information from Small-Angle Scattering Experiments. *J. Appl. Crystallogr.* **1979**, *12*, 166−175.
(66) Osseo-Asare, K. Enhanced Solvent Extraction with Water-in-Oil Microemulsions. *Sep. Sci. Technol.* **1988**, *23*, 1269−1284.
(67) du Preez, J. G. H.; Sumter, N. M.; Viviers, C.; Rohwer, H. E.; van Brecht, B. J. A. M. In *Emerging Separation Technologies for Metals II*; Bautista, R. G., Ed.; The Minerals, Metals & Materials Society: Warrendale, PA, 1996; pp 265−278.
(68) Laing, M. In *Coordination Chemistry. A Century of Progress*; Kauffman, G. B., Ed.; ACS Symp. Series 565; American Chemical Society: Washington, DC, 1994; Vol. *565*, pp 382−394.